Article:
Zhang, B. and Liu, W. (2018) Multi-carrier based phased antenna array design for directional modulation. IET Microwaves, Antennas and Propagation, 12 (5). pp. 765-772. ISSN: 1751-8725

https://doi.org/10.1049/iet-map.2017.0505

IET Microwaves, Antennas & Propagation

Research Article

IET Journals
The Institution of Engineering and Technology

Multi-carrier based phased antenna array design for directional modulation

ISSN 1751-8725
Received on 16th June 2017
Revised 12th September 2017
Accepted on 22nd November 2017
doi: 10.1049/iet-map.2017.0505
www.ietdl.org

Bo Zhang[1], *Wei Liu*[1] ✉

[1]*Communications Research Group, Department of Electronic and Electrical Engineering, University of Sheffield, Sheffield S1 4ET, UK*
✉ *E-mail: w.liu@sheffield.ac.uk*

Abstract: Directional modulation (DM) has been developed based on narrowband antenna arrays, which can form the desired constellation values in the directions of interest while scrambling the values and simultaneously maintaining a magnitude response as low as possible in other directions. In this study, for the first time, the authors develop a multi-carrier based DM framework using antenna arrays, where simultaneous data transmission over multiple frequencies can be achieved, so that a much higher data rate can be obtained. In addition, such a framework allows possible frequency division based multi-user access to the system and also provides the flexibility of using different modulation schemes at different frequencies. Then, they study the antenna location optimisation problem for multi-carrier based DM using a compressive sensing based approach by employing the group sparsity concept. Examples are provided for both the design of weight coefficients and the optimisation of antenna locations.

1 Introduction

Directional modulation (DM) is a physical layer security technique using advanced antenna and array design methods, which aims to keep the desired constellation values in the directions of interest while scrambling the values and simultaneously maintaining a magnitude response as low as possible in other directions.

It was first introduced in [1, 2] as a near-field modulation technique using reflector switching. Then, a four-element reconfigurable antenna array was introduced in [3] to achieve DM by switching elements for each symbol to change its amplitude and phase of the element radiation pattern. In [4], a method called dual-beam DM was introduced, where the in-phase and quadrature signals are transmitted by different antennas, instead of the same antenna that is used for traditional transmission. Phased arrays were introduced in [5] to realise DM and they were further investigated in [6–8]. In [9], a new DM approach was proposed, where the radiation pattern is separated into information pattern and interference pattern through far-field null steering to control array excitations. In [10], a design of far-field radiation pattern templates was developed for DM. Recently, a time modulation technique was proposed for DM to form a four-dimensional antenna array [11].

However, all these works are based on the assumption that the information is transmitted at one single frequency, which is not an efficient way to use the available spectrum. In this work, borrowing the idea of multi-carrier based transmission for traditional wireless communication systems [12–15], we develop a novel multi-carrier based DM structure for antenna arrays, which can be implemented efficiently by the inverse discrete Fourier transform (IDFT). There are mainly three advantages for the proposed multi-carrier based DM: the first is that we can transmit multiple low rate data streams in parallel to achieve a much higher overall data rate, extending the use of DM effectively and efficiently to a wider bandwidth; the second advantage is that we can assign different carriers to different users allowing possible frequency division multi-user access, where the users can be located at the same directions or different directions and in the latter case, we can design the beam pointing to different directions at different frequencies; the third advantage is that it provides the flexibility of using different modulation schemes at different carrier frequencies.

First, we will extend the traditional single-carrier design for DM to the multi-carrier case for a given array geometry. Then we study the antenna location optimisation problem for multi-carrier based DM using a compressive sensing (CS) based approach by extending the formulation developed for narrowband sparse arrays in [16]. For the single-carrier case, we only need to find a common set of antenna locations for all constellation points. For the multi-carrier structure, since more than one carrier frequency are used, a common solution only for all constellation points at one frequency is not enough, and we need to find a common set of optimised antenna locations for all modulation symbols at all carrier frequencies instead.

The remaining part of this paper is structured as follows. A review of the traditional DM structure is given in Section 2, followed by the proposed multi-carrier based structure and its design with a given array geometry. The CS-based antenna location optimisation method for multi-carrier based DM arrays is presented in Section 3. Design examples are provided in Section 4, with conclusions drawn in Section 5.

2 Proposed structure for multi-carrier based directional modulation

2.1 Review of DM with a single carrier

A narrowband linear array for transmit beamforming is shown in Fig. 1 [17], consisting of N equally spaced omnidirectional antennas with the spacing from the first antenna to its subsequent antennas represented by d_n for $n = 1, \ldots, N-1$, where the transmission angle $\theta \in [0^{\circ}, 180^{\circ}]$. The output signal and weight coefficient for each antenna are, respectively, denoted by x_n and w_n, $n = 0, \ldots, N-1$. The steering vector of the array is a function of angular frequency ω and transmission angle θ, given by

$$\boldsymbol{s}(\omega, \theta) = [1, \mathrm{e}^{\mathrm{j}\omega d_1 \cos\theta/c}, \ldots, \mathrm{e}^{\mathrm{j}\omega d_{N-1} \cos\theta/c}]^{\mathrm{T}}, \tag{1}$$

where $\{\cdot\}^{\mathrm{T}}$ is the transpose operation, and c is the speed of propagation. The vector of weight coefficients for their corresponding antennas is represented by $\boldsymbol{w}$ with

$$\boldsymbol{w} = [w_0, w_1, \ldots, w_{N-1}]^{\mathrm{T}}. \tag{2}$$

Then, the beam response of the array is given by

$$p(\theta) = \boldsymbol{w}^{\mathrm{H}} \boldsymbol{s}(\omega, \theta), \tag{3}$$

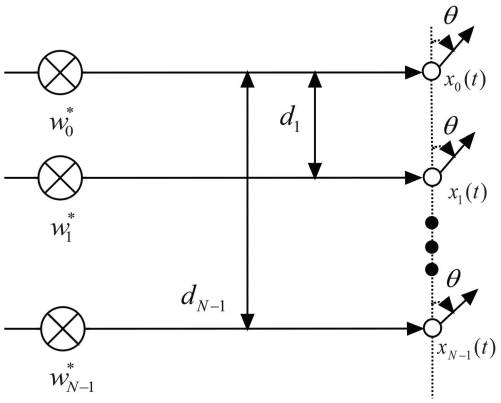

Fig. 1 *Narrowband transmit beamforming structure*

where $\{\cdot\}^{\mathrm{H}}$ represents the Hermitian transpose.

For M-ary signalling, such as multiple phase shift keying, there are M sets of desired array responses $p_m(\theta)$, with a corresponding weight vector $\boldsymbol{w}_m = [w_{m,0}, \ldots, w_{m,N-1}]^{\mathrm{T}}$, $m = 0, , \ldots, M-1$. Each desired response $p_m(\theta)$ is further split into two regions according to the direction of θ: the mainlobe $\boldsymbol{p}_{m,\mathrm{ML}}$ and the sidelobe $\boldsymbol{p}_{m,\mathrm{SL}}$. The mainlobe will have the desired response representing the corresponding modulation symbol, while the sidelobe has a low gain with a scrambled phase response. For r sample points in the mainlobe and $R-r$ sample points in the sidelobe, we have

$$\begin{aligned}\boldsymbol{p}_{m,\mathrm{SL}} &= [p_m(\theta_0), p_m(\theta_1), \ldots, p_m(\theta_{R-r-1})]\\ \boldsymbol{p}_{m,\mathrm{ML}} &= [p_m(\theta_{R-r}), p_m(\theta_{R-r+1}), \ldots, p_m(\theta_{R-1})]\,.\end{aligned} \tag{4}$$

All constellation points for a fixed θ share the same steering vector, and we put all the $R-r$ steering vectors at the sidelobe region into an $N \times (R-r)$ matrix $\boldsymbol{S}_{\mathrm{SL}}$, and the r steering vectors at the mainlobe direction into an $N \times r$ matrix, denoted by $\boldsymbol{S}_{\mathrm{ML}}$. For the mth constellation point, its corresponding weight coefficients can be found by solving the following constrained optimisation problem:

$$\begin{aligned}&\min \qquad \|\boldsymbol{p}_{m,\mathrm{SL}} - \boldsymbol{w}_m^{\mathrm{H}}\boldsymbol{S}_{\mathrm{SL}}\|_2\\ &\text{subject to} \quad \boldsymbol{w}_m^{\mathrm{H}}\mathbf{S}_{\mathrm{ML}} = \boldsymbol{p}_{m,\mathrm{ML}},\end{aligned} \tag{5}$$

where $\|\cdot\|_2$ denotes the l_2 norm.

2.2 Proposed multi-carrier DM structure with a given array geometry

The proposed multi-carrier based transmit beamforming array structure for DM is shown in Fig. 2, where each antenna is associated with multiple frequency-dependent weight coefficients $w_{n,q}$, for $n = 0, \ldots, N-1$ and $q = 0, \ldots, Q-1$. The beamformer output $x_n(t)$ can be represented as follows:

$$\begin{aligned}x_n(t) &= \sum_{q=0}^{Q-1} w_{n,q}^* \mathrm{e}^{\mathrm{j}2\pi(f_0 + (-(Q/2)+q)\Delta f)t}\\ &= \sum_{q=0}^{Q-1} w_{n,q}^* \mathrm{e}^{\mathrm{j}2\pi(-(Q/2)+q)\Delta f t} \times \mathrm{e}^{\mathrm{j}2\pi f_0 t}\end{aligned} \tag{6}$$

where f_0 represents the carrier frequency and Δf denotes the subcarrier spacing.

To derive a discrete baseband representation of the structure, we omit the carrier frequency f_0, and substitute $t = kt_s$ into (6) for $k = 0, 1, \ldots, Q-1$ and $t_s = (1/\Delta f \times Q)$ ($\Delta f \times Q$ represents the bandwidth of the baseband signal from $[-(Q/2)\times\Delta f, (Q/2)\times\Delta f]$). Therefore, the discrete baseband signal is given by

$$\begin{aligned}x_n(k) &= \sum_{q=0}^{Q-1} w_{n,q}^* \mathrm{e}^{\mathrm{j}2\pi(-(Q/2)+q)\Delta f k t_s}\\ &= \sum_{q=0}^{Q-1} w_{n,q}^* \mathrm{e}^{\mathrm{j}2\pi(-(Q/2)+q)\Delta f k (1/\Delta f Q)}\\ &= Q \times \frac{1}{Q}\sum_{q=0}^{Q-1} w_{n,q}^* \mathrm{e}^{\mathrm{j}2\pi(-(Q/2)+q)(k/Q)}, \quad k = 0, 1, \ldots, Q-1\end{aligned} \tag{7}$$

where $(1/Q)\sum_{q=0}^{Q-1} w_{n,q}^* \mathrm{e}^{\mathrm{j}2\pi(-(Q/2)+q)(k/Q)}$ is the IDFT expression of $w_{n,q}^*$. Therefore, mathematically modulating on each subcarrier and then adding them together is equivalent to taking an IDFT. The outputs of IDFT are then followed by a parallel to serial converter (P/S) with the time interval t_s between adjacent samples and a digital-to-analogue converter (D/A). Finally, the multiple baseband signals are modulated to their corresponding carrier frequency and transmitted through the antennas. The new multi-carrier structure is represented in Fig. 3.

To have a beam pointing to a certain direction, the steering vector for the qth frequency is given by

$$\begin{aligned}\mathbf{s}(\omega_q, \theta) &= [1, \mathrm{e}^{\mathrm{j}\omega_q\tau_1}, \ldots, \mathrm{e}^{\mathrm{j}\omega_q\tau_{N-1}}]^{\mathrm{T}}\\ &= [1, \mathrm{e}^{\mathrm{j}2\pi(f_0 + (-\frac{Q}{2}+q)\Delta f)\tau_1}, \ldots,\\ &\qquad \mathrm{e}^{\mathrm{j}2\pi(f_0 + (-\frac{Q}{2}+q)\Delta f)\tau_{N-1}}]^{\mathrm{T}}.\end{aligned} \tag{8}$$

where τ_n for $n = 1, \ldots, N-1$ is the propagation advance for the signal from antenna n to antenna 0 and is a function of transmission angle θ, represented by $((d_n\cos(\theta))/c)$. Then, the beam response of the array at the qth frequency is formulated as follows:

$$p(\omega_q, \theta) = \boldsymbol{w}(\omega_q)^{\mathrm{H}}\boldsymbol{s}(\omega_q, \theta), \tag{9}$$

and $\boldsymbol{w}(\omega_q)$ is the weight vector at the qth frequency, given by

$$\boldsymbol{w}(\omega_q) = [w_{0,q}, w_{1,q}, \ldots, w_{N-1,q}]^{\mathrm{T}}. \tag{10}$$

Similarly, for M-ary signalling, we define $p_m(\omega_q, \theta)$ as the desired array response to the mth constellation point at the q-th frequency for $m = 0, \ldots, M-1$ and $q = 0, \ldots, Q-1$, and then divide them into $\boldsymbol{p}_m(\omega_q, \theta_{\mathrm{ML}})$ (beam responses at the main lobe directions) and $\boldsymbol{p}_m(\omega_q, \theta_{\mathrm{SL}})$ (beam responses over the side lobe regions) in the same way as in (4), according to the direction of θ, where

$$\begin{aligned}\boldsymbol{p}_m(\omega_q, \theta_{\mathrm{SL}}) &= [p_m(\omega_q, \theta_0), p_m(\omega_q, \theta_1), \ldots,\\ &\qquad p_m(\omega_q, \theta_{R-r-1})]\\ \boldsymbol{p}_m(\omega_q, \theta_{\mathrm{ML}}) &= [p_m(\omega_q, \theta_{R-r}), p_m(\omega_q, \theta_{R-r+1}), \ldots,\\ &\qquad p_m(\omega_q, \theta_{R-1})]\ .\end{aligned} \tag{11}$$

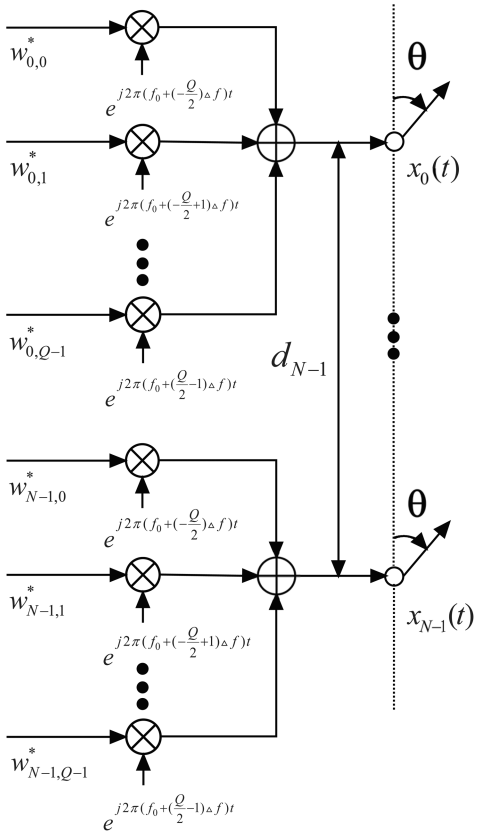

Fig. 2 *Proposed multi-carrier transmit beamforming structure for DM*

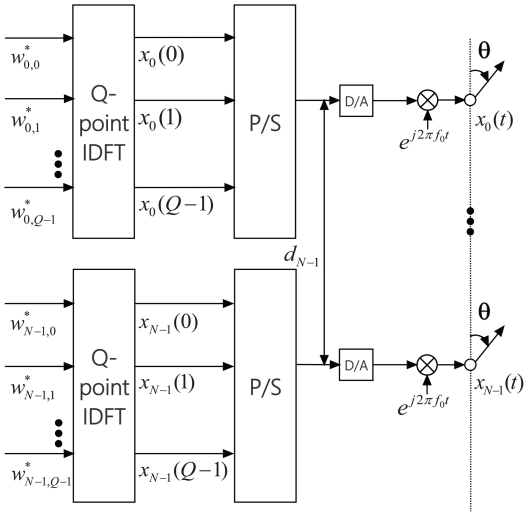

Fig. 3 *Proposed multi-carrier transmit beamforming structure for DM represented by IDFT*

The corresponding weight vector is represented by $\boldsymbol{w}_m(\omega_q) = [w_{m,0,q}, \ldots, w_{m,N-1,q}]^{\mathrm{T}}$. Moreover, $\boldsymbol{S}(\omega_q, \theta_{\mathrm{SL}})$ is an $N \times (R-r)$ matrix including all steering vectors at sidelobe regions at the qth frequency, and the steering vector in the mainlobe θ_{ML} is an $N \times r$ matrix, denoted by $\boldsymbol{S}(\omega_q, \theta_{\mathrm{ML}})$.

For the mth constellation point at the qth carrier frequency based on a given geometry, its corresponding weight coefficients can be obtained by solving the following constrained minimisation problem:

$$\begin{aligned} &\min && ||\boldsymbol{p}_m(\omega_q, \theta_{\mathrm{SL}}) - \boldsymbol{w}_m(\omega_q)^{\mathrm{H}}\boldsymbol{S}(\omega_q, \theta_{\mathrm{SL}})||_2 \\ &\text{subject to} && \boldsymbol{w}_m(\omega_q)^{\mathrm{H}}\boldsymbol{S}(\omega_q, \theta_{\mathrm{ML}}) = \boldsymbol{p}_m(\omega_q, \theta_{\mathrm{ML}}) . \end{aligned} \tag{12}$$

The objective function and constraint in (12) ensure a minimum difference between the desired and designed responses in the sidelobe, and a desired constellation value to the mainlobe or the direction of interest. To ensure that the constellation is scrambled in the sidelobe regions, the phase of the desired response $\boldsymbol{w}_m(\omega_q)^{\mathrm{H}}\boldsymbol{S}(\omega_q, \theta_{\mathrm{SL}})$ at different sidelobe directions can be randomly generated

$$\begin{aligned} \boldsymbol{w}_m(\omega_q) = \boldsymbol{R}^{-1}(&\boldsymbol{S}(\omega_q, \theta_{\mathrm{SL}})\boldsymbol{p}_m^{\mathrm{H}}(\omega_q, \theta_{\mathrm{SL}}) - \boldsymbol{S}(\omega_q, \theta_{\mathrm{ML}}) \\ &\times ((\boldsymbol{S}^{\mathrm{H}}(\omega_q, \theta_{\mathrm{ML}})\boldsymbol{R}^{-1}\mathbf{S}(\omega_q, \theta_{\mathrm{ML}}))^{-1}(\boldsymbol{S}^{\mathrm{H}}(\omega_q, \theta_{\mathrm{ML}}) \\ &\times \boldsymbol{R}^{-1}\boldsymbol{S}(\omega_q, \theta_{\mathrm{SL}})\boldsymbol{p}_m^{\mathrm{H}}(\omega_q, \theta_{\mathrm{SL}}) - \boldsymbol{p}^{\mathrm{H}}(\omega_q, \theta_{\mathrm{ML}})))) . \end{aligned} \tag{13}$$

The problem in (12) can be solved by the method of Lagrange multipliers and the optimum value for the weight vector $\boldsymbol{w}_m(\omega_q)$ is given in (13), where $\boldsymbol{R} = \boldsymbol{S}(\omega_q, \theta_{\mathrm{SL}})\boldsymbol{S}^{\mathrm{H}}(\omega_q, \theta_{\mathrm{SL}})$.

3 Location optimisation of array antennas for multi-carrier based DM

Equation (12) is only for designing the DM coefficients for a given set of antenna locations. In practice, we may need to optimise the antenna locations to achieve an even lower cost function in (12) or reduce the number of required antennas for a similar level of cost function minimisation result. This is a traditional sparse antenna array design problem [18, 19]. Many methods have been proposed for the design of a general sparse antenna array, including the genetic algorithm [20–22], simulated annealing [23] and CS [17, 24–28], and in the context of single-carrier DM, it has been studied using CS-based methods in our recent publication [16].

For CS-based sparse DM array design with a single carrier [16], a given aperture represented by d_{N-1}, as shown in Fig. 1, is densely sampled with a large number (N) of potential antennas, where the values of d_n, for $n = 1, 2, \ldots, N-1$, are selected to give a uniform grid. Through selecting the minimum number of non-zero valued weight coefficients to generate a response close to the desired one described in (5), sparseness is achieved in the resultant design. In other words, if a weight coefficient is zero-valued, the corresponding antenna will be deemed inactive and therefore can be removed, leading to a sparse result.

Following this idea, for the multi-carrier structure in Fig. 3, where each antenna is connected to multiple frequency-dependent weight coefficients, we could formulate the problem for the mth constellation point at the qth carrier frequency as follows:

$$\begin{aligned} \min \quad & ||\boldsymbol{w}_m(\omega_q)||_1 \\ \text{subject to} \quad & ||\boldsymbol{p}_m(\omega_q, \theta_{\text{SL}}) - \boldsymbol{w}_m(\omega_q)^{\text{H}} \boldsymbol{S}(\omega_q, \theta_{\text{SL}})||_2 \le \alpha \\ & \boldsymbol{w}_m(\omega_q)^{\text{H}} \boldsymbol{S}(\omega_q, \theta_{\text{ML}}) = \boldsymbol{p}_m(\omega_q, \theta_{\text{ML}}) . \end{aligned} \tag{14}$$

where $||\cdot||_1$ is the l_1 norm, used as an approximation to the l_0 norm, and α is the allowed difference between the desired and designed responses.

However, the solution to (14) cannot guarantee the same set of active antenna positions for all constellation points at all frequencies. This means an antenna cannot be removed if the corresponding weight coefficients for all constellation points at all frequencies are not all zero-valued; in other words, to remove an antenna, we need all elements in the vector $\tilde{\boldsymbol{w}}_n$ to be zero-valued or $||\tilde{\boldsymbol{w}}_n||_2 = 0$, where

$$\begin{aligned} \tilde{\boldsymbol{w}}_n = [& w_{0,n,0}, w_{1,n,0}, \ldots, w_{M-1,n,0}, \\ & w_{0,n,1}, \ldots, w_{M-1,n,1}, \ldots, w_{M-1,n,Q-1}], \end{aligned} \tag{15}$$

Here $w_{m,n,q}$ represents the weight coefficient corresponding to the nth antenna location for the mth constellation point at the qth frequency. Then, to reduce the number of elements for an N-element antenna array, we gather all $||\tilde{\boldsymbol{w}}_n||_2$ for $n = 0, \ldots, N-1$ to form a vector $\hat{\boldsymbol{w}}$, given by

$$\hat{\boldsymbol{w}} = [||\tilde{\boldsymbol{w}}_0||_2, ||\tilde{\boldsymbol{w}}_1||_2, \ldots, ||\tilde{\boldsymbol{w}}_{N-1}||_2]^{\text{T}}, \tag{16}$$

and $\min ||\hat{\boldsymbol{w}}||_1$ represents the minimum number of non-zero valued $||\tilde{\boldsymbol{w}}_n||_2$ or the sparsest antenna array. This idea is called group sparsity [29], which is used here for finding a common set of active antenna locations for all constellation points at all Q frequencies. Moreover, we need to impose DM constraints at all frequencies. Therefore, we first construct the following matrices:

$$\boldsymbol{W}(\omega_q) = [\boldsymbol{w}_0(\omega_q), \boldsymbol{w}_1(\omega_q), \ldots, \boldsymbol{w}_{M-1}(\omega_q)] \tag{17}$$

$$\begin{aligned} \boldsymbol{P}_{\text{SL}}(\omega_q, \theta_{\text{SL}}) = [& \boldsymbol{p}_0(\omega_q, \theta_{\text{SL}}), \boldsymbol{p}_1(\omega_q, \theta_{\text{SL}}), \ldots, \boldsymbol{p}_{M-1}(\omega_q, \theta_{\text{SL}})]^{\text{T}} \\ & \boldsymbol{p}_{M-1}(\omega_q, \theta_{\text{SL}})]^{\text{T}} \end{aligned} \tag{18}$$

$$\begin{aligned} \boldsymbol{p}_{\text{ML}}(\omega_q, \theta_{\text{ML}}) = [& \boldsymbol{p}_0(\omega_q, \theta_{\text{ML}}), \boldsymbol{p}_1(\omega_q, \theta_{\text{ML}}), \ldots, \\ & \boldsymbol{p}_{M-1}(\omega_q, \theta_{\text{ML}})]^{\text{T}} \end{aligned} \tag{19}$$

for $q = 0, 1, \ldots, Q-1$. Then, based on the above matrices, a series of block diagonal ones are formed as follows:

$$\boldsymbol{W} = \text{blkdiag}\{\boldsymbol{W}(\omega_0), \boldsymbol{W}(\omega_1), \ldots, \boldsymbol{W}(\omega_{Q-1})\} \tag{20}$$

$$\begin{aligned} \boldsymbol{P}_{SL} = \text{blkdiag}\{& \boldsymbol{P}_{\text{SL}}(\omega_0, \theta_{\text{SL}}), \boldsymbol{P}_{\text{SL}}(\omega_1, \theta_{\text{SL}}), \\ & \ldots, \boldsymbol{P}_{\text{SL}}(\omega_{Q-1}, \theta_{\text{SL}})\} \end{aligned} \tag{21}$$

$$\begin{aligned} \boldsymbol{P}_{\text{ML}} = \text{blkdiag}\{& \boldsymbol{p}_{\text{ML}}(\omega_0, \theta_{\text{ML}}), \boldsymbol{p}_{\text{ML}}(\omega_1, \theta_{\text{ML}}), \\ & \ldots, \boldsymbol{p}_{\text{ML}}(\omega_{Q-1}, \theta_{\text{ML}})\} \end{aligned} \tag{22}$$

$$\begin{aligned} \boldsymbol{S}_{\text{SL}} = \text{blkdiag}\{& \boldsymbol{S}(\omega_0, \theta_{\text{SL}}), \boldsymbol{S}(\omega_1, \theta_{\text{SL}}), \\ & \ldots, \boldsymbol{S}(\omega_{Q-1}, \theta_{\text{SL}})\} \end{aligned} \tag{23}$$

$$\begin{aligned} \boldsymbol{S}_{\text{ML}} = \text{blkdiag}\{& \boldsymbol{s}(\omega_0, \theta_{\text{ML}}), \boldsymbol{s}(\omega_1, \theta_{\text{ML}}), \\ & \ldots, \boldsymbol{s}(\omega_{Q-1}, \theta_{\text{ML}})\} . \end{aligned} \tag{24}$$

Then, the l_1 norm minimisation for sparse DM array design can be formulated as

$$\begin{aligned} \min \quad & ||\hat{\boldsymbol{w}}||_1 \quad \text{subjectto} \quad ||\boldsymbol{P}_{\text{SL}} - \boldsymbol{W}^{\text{H}} \boldsymbol{S}_{\text{SL}}||_2 \le \alpha \\ & \boldsymbol{W}^{\text{H}} \boldsymbol{S}_{\text{ML}} = \boldsymbol{P}_{\text{ML}} . \end{aligned} \tag{25}$$

As the reweighted l_1 norm minimisation has a closer approximation to the l_0 norm [30–32], we can further modify (25) into the reweighted form in a similar way as in [16]. For the reweighted design, at the ith iteration, the above formulations (25) become

$$\begin{aligned} \min \quad & \sum_{n=1}^{N} \delta_n^i ||\tilde{\boldsymbol{w}}_n^i||_2 \\ \text{subjectto} \quad & ||\boldsymbol{P}_{\text{SL}} - (\boldsymbol{W}^i)^{\text{H}} \boldsymbol{S}_{\text{SL}}||_2 \le \alpha \\ & (\boldsymbol{W}^i)^{\text{H}} \boldsymbol{S}_{\text{ML}} = \boldsymbol{P}_{\text{ML}} , \end{aligned} \tag{26}$$

where the superscript i indicates the ith iteration, and δ_n is the reweighting term for the nth row of coefficients, given by $\delta_n^i = \left(||\tilde{\boldsymbol{w}}_n^{i-1}||_2 + \gamma\right)^{-1}$. Here $\gamma > 0$ is required to provide numerical stability to prevent δ_n^i becoming infinity at the current iteration if the value of a weight coefficient is zero at the previous iteration, and it is chosen to be slightly less than the minimum weight coefficient that will be implemented in the final design (i.e. the value below which the associated antenna will be considered inactive and therefore removed from the obtained design result), where $\delta_n^i ||\tilde{\boldsymbol{w}}_n^i||_2 = ((||\tilde{\boldsymbol{w}}_n^i||_2)/(||\tilde{\boldsymbol{w}}_n^i||_2 + \gamma))$.

The iteration process is described as follows:

(i) For the first iteration ($i = 1$), calculate the initial value $||\tilde{\boldsymbol{w}}_n||_2$ by solving (25).

(ii) Set $i = i + 1$. Use the value of the last $||\tilde{\boldsymbol{w}}_n^{i-1}||_2$ to calculate δ_n^i, and then find $\boldsymbol{W}^i$ and $||\tilde{\boldsymbol{w}}_n^i||_2$ by solving the problem in (26).

(iii) Repeat step (ii) until the positions of non-zero values of the weight coefficients do not change any more for some number of iterations.

The problem in (26) can be solved using CVX, a package for specifying and solving convex programs [33, 34].

4 Design examples

In this section, several representative design examples are provided to show the working of the proposed multi-carrier based DM array structure and the performance of the location-optimised sparse array in comparison with a standard ULA.

Without loss of generality, we assume the mainlobe direction is $\theta_{\text{ML}} = 90^\circ$ and the sidelobe regions are $\theta_{SL} \in [0^\circ, 85^\circ] \cup [95^\circ, 180^\circ]$, sampled every 1° in our design. Consider a standard Wi-Fi

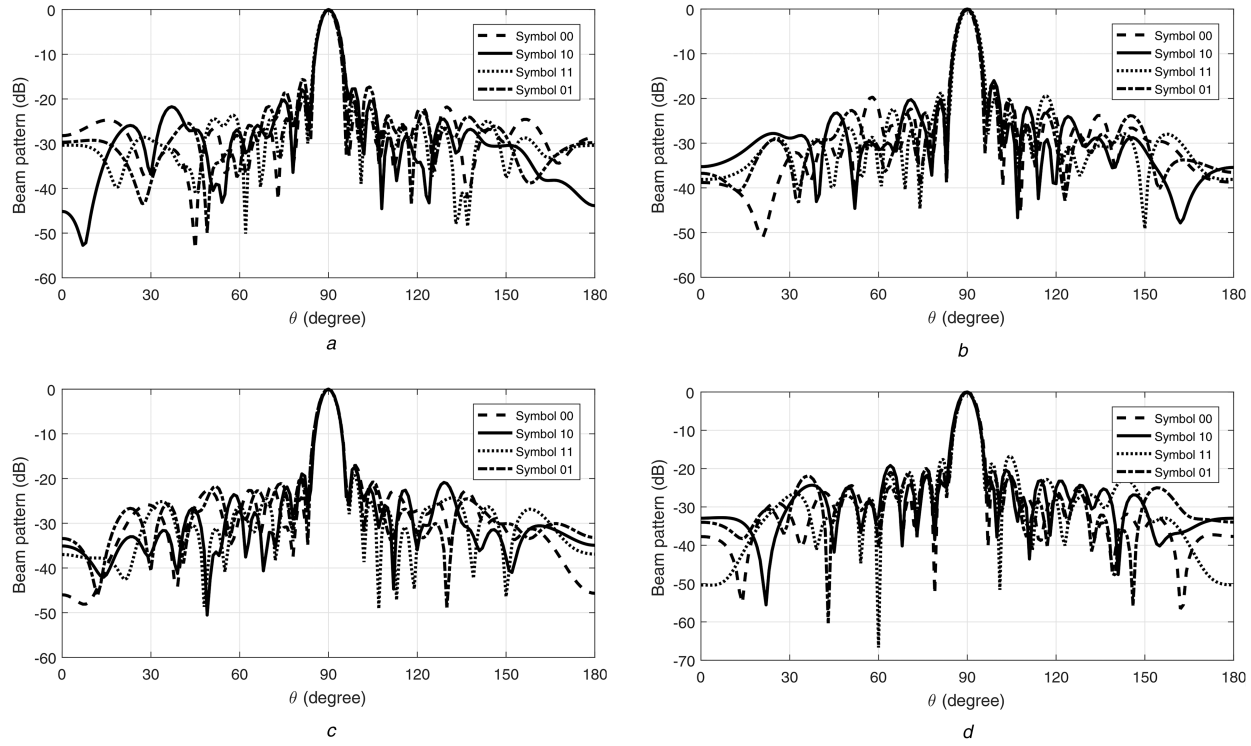

Fig. 4 *Resultant beam responses based on the design (12) at* ***(a)*** $f_0 - 4\Delta f$, ***(b)*** $f_0 - 2\Delta f$, ***(c)*** f_0, ***(d)*** $f_0 + 2\Delta f$

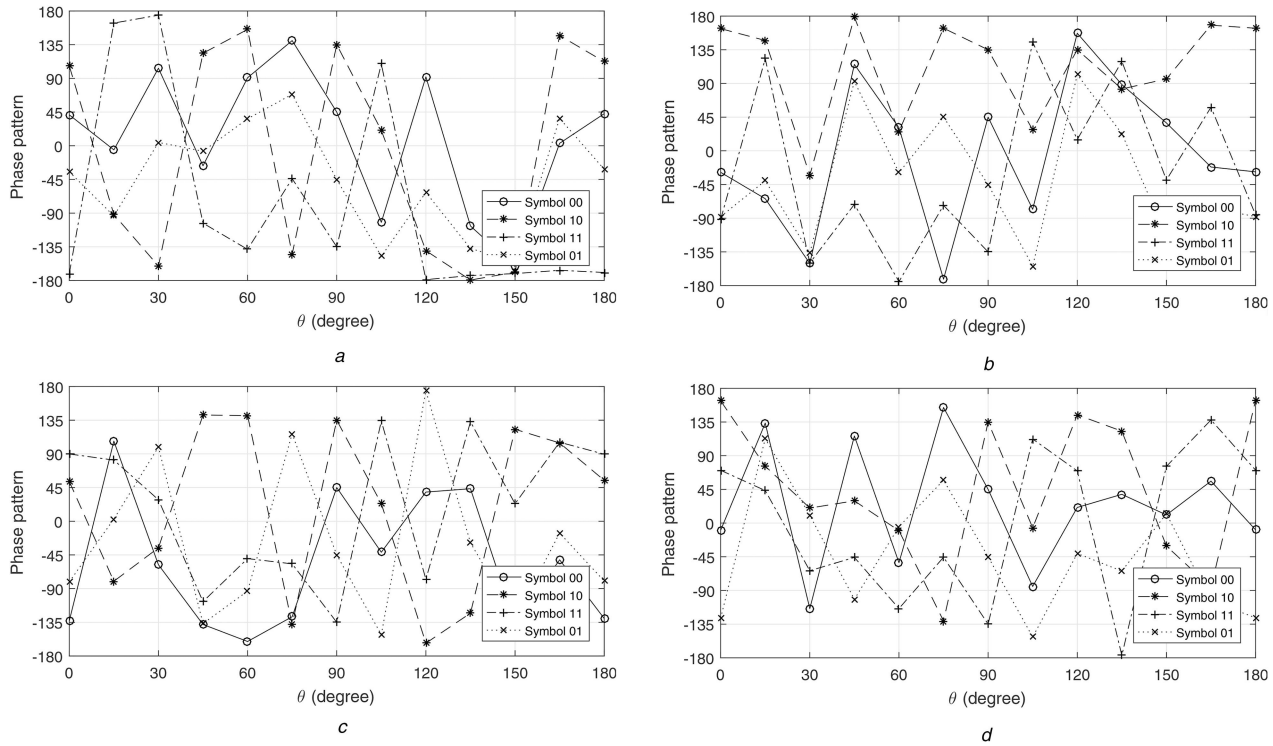

Fig. 5 *Resultant phase patterns based on the design (12) at* ***(a)*** $f_0 - 4\Delta f$, ***(b)*** $f_0 - 2\Delta f$, ***(c)*** f_0, ***(d)*** $f_0 + 2\Delta f$

transmission. The carrier frequency f_0 is set to 2.4 GHz, with a bandwidth of 2.5 MHz, split into eight frequencies (eight-point IDFT). The desired response is a value of one (magnitude) with 90° phase shift at the mainlobe [quadrature phase shift keying (QPSK)] and a value of 0.1 (magnitude) with random phase shifts over the sidelobe regions for each frequency.

To have a fair comparison, we first obtain the DM result using the method in (12) based on a 21-element ULA with a spacing of half-wavelength at the highest frequency. Based on the design result, we then calculate the error norm between the designed and the desired responses and its value represented by α is then used in the sparse array design as the threshold.

4.1 Design example with a given array geometry

The resultant beam patterns using (12) at frequencies $f_0 - 4\Delta f$, $f_0 - 2\Delta f$, f_0, $f_0 + 2\Delta f$ are shown in Figs. 4*a–d*, and the corresponding phase patterns are displayed in Figs. 5*a–d*. The beam and phase patterns on frequencies $f_0 - 3\Delta f$, $f_0 - \Delta f$, $f_0 + \Delta f$, $f_0 + 3\Delta f$ are not shown as they have the same features as

Table 1 Resultant weight coefficients for $m = 0$ (symbol 00) at the frequency 2.39875 GHz based on (12)

n	Weights	n	Weights
1	0.0203 – j0.0189	12	0.0437 – j0.0455
2	0.0212 – j0.0274	13	0.0490 – j0.0438
3	0.0334 – j0.0206	14	0.0388 – j0.0459
4	0.0307 – j0.0258	15	0.0289 – j0.0368
5	0.0390 – j0.0411	16	0.0366 – j0.0344
6	0.0361 – j0.0359	17	0.0181 – j0.0431
7	0.0462 – j0.0368	18	0.0248 – j0.0288
8	0.0440 – j0.0451	19	0.0231 – j0.0167
9	0.0481 – j0.0413	20	0.0236 – j0.0197
10	0.0400 – j0.0384	21	0.0087 – j0.0217
11	0.0528 – j0.0455		

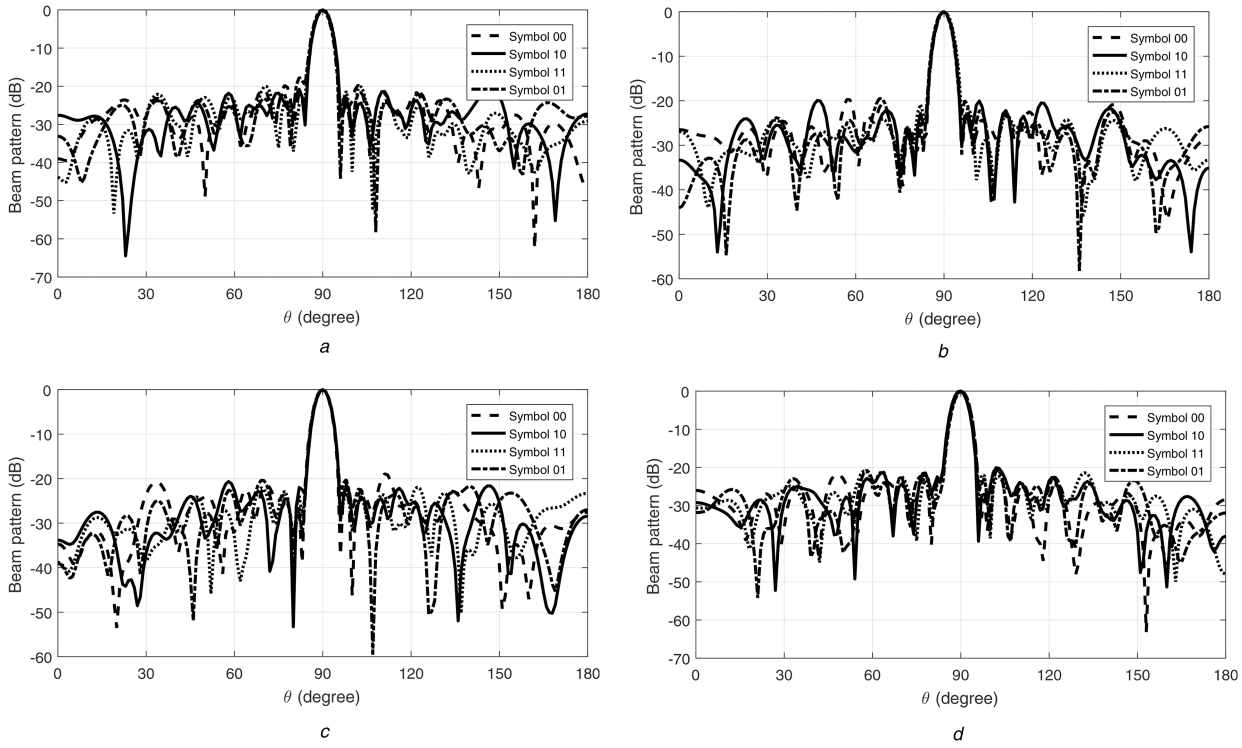

Fig. 6 *Resultant beam responses based on the design (26) at* ***(a)*** $f_0 - 4\Delta f$, ***(b)*** $f_0 - 2\Delta f$, ***(c)*** f_0, ***(d)*** $f_0 + 2\Delta f$

the aforementioned figures, where all main beams are exactly pointed to 90° with a reasonable sidelobe level, and the designed phase at the mainlobe direction ($\theta = 90°$) for the constellation points follows the standard QPSK constellation, i.e. symbols '00', '10', '11', '01' correspond to 45°, 135°, −45° and −135°, respectively, while for the rest of the θ angles, phases of these symbols are random and their phase difference are scrambled, demonstrating that DM has been achieved effectively. The resultant weight coefficients for $m = 0$ (symbol 00) at the frequency 2.39875 GHz is shown in Table 1.

4.2 Design example with antenna location optimisation

With the same value of error norm α obtained from the above ULA design case, we have set the maximum aperture to be 15λ with 150 equally spaced potential antennas for the multi-carrier structure based sparse array design. Moreover, $\gamma = 0.001$ was set to indicate that antennas associated with a weight value smaller than 0.001 is considered inactive.

For the reweighted l_1 norm minimisation method in (26), the resultant number of active antennas is 16, with an average spacing of 9.64 cm, as shown in Table 2. Figs. 6*a–d* show the beam patterns and Figs. 7*a–d* display the phase patterns at frequencies $f_0 - 4\Delta f$, $f_0 - 2\Delta f$, f_0 and $f_0 + 2\Delta f$, all indicating a satisfactory design result. The beam and phase patterns for other frequencies have a similar performance as the above frequencies.

A performance comparison between the ULA design and the reweighted design is summarised in Table 3, where the result using direct l_1 norm minimisation in (25) (i.e. without reweighted iteration) is also included. We can see that they all have a very similar sidelobe level; however, the number of antennas required after location optimisation has been reduced by five using the reweighted design. Although the method in (25) also gives a sparse solution, with an adjacent antenna spacing larger than half wavelength, the number of antennas is increased from 21 to 24 (therefore with a much reduced sidelobe error), highlighting the need for the proposed reweighted design in (26).

5 Conclusions

A multi-carrier based antenna array structure for DM has been proposed for the first time, where a baseband implementation similar to the classic OFDM structure in wireless communications is derived. Then we studied the antenna location optimisation problem in this context and a class of CS-based design methods were developed. The key is to find a common set of sparse result for all modulation symbols at all frequencies using the concept of group sparsity. As shown in the provided design examples, in the context of DM, the sparse design has achieved a main lobe

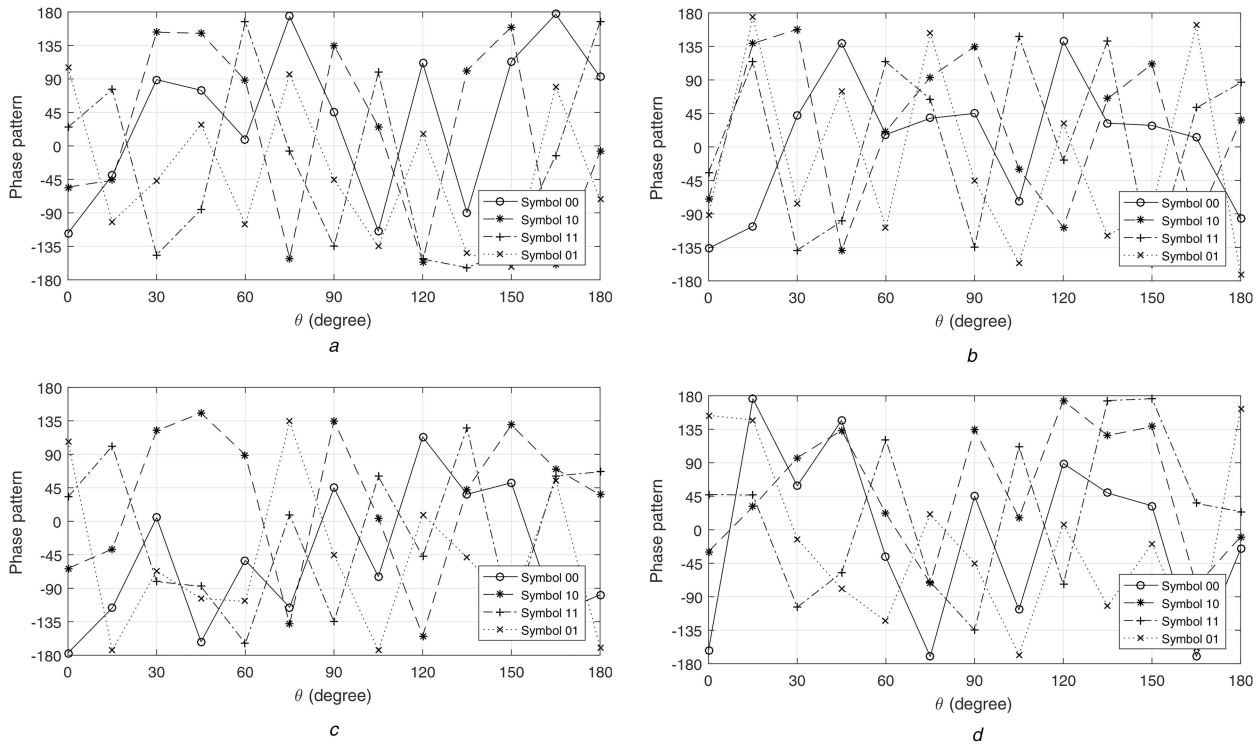

Fig. 7 *Resultant phase patterns based on the design (26) at* ***(a)*** $f_0 - 4\Delta f$, ***(b)*** $f_0 - 2\Delta f$, ***(c)*** f_0, ***(d)*** $f_0 + 2\Delta f$

Table 2 Optimised antenna locations based on the reweighted l_1 norm design

n	d_n, cm	n	d_n, cm	n	d_n, cm
1	33.96	7	89.31	13	145.92
2	44.03	8	100.63	14	155.98
3	55.35	9	110.70	15	167.30
4	66.67	10	119.50	16	178.62
5	75.47	11	124.53		
6	77.99	12	134.60		

Table 3 Summary of the design results

	ULA	l_1	Reweighted l_1
antenna number	21	24	16
aperture, cm	124.95	187.43	144.66
average spacing, cm	6.25	8.15	9.64
$\|\|\boldsymbol{P}_{\mathrm{SL}} - \boldsymbol{W}^{\mathrm{H}}\boldsymbol{S}_{\mathrm{SL}}\|\|_2$	7.631	7.088	7.6965

pointing to the desired direction with scrambled phases in other directions. In particular, the design can provide a sparse solution as expected, using less number of antennas with a satisfactory performance compared to the ULA design case.

6 References

[1] Babakhani, A., Rutledge, D. B., Hajimiri, A.: 'Transmitter architectures based on near-field direct antenna modulation', *IEEE J. Solid-State Circuits*, 2008, **43**, (12), pp. 2674–2692

[2] Babakhani, A., Rutledge, D.B., Hajimiri, A.: 'Near-field direct antenna modulation', *IEEE Microw. Mag.*, 2009, **10**, (1), pp. 36–46

[3] Daly, M.P., Bernhard, J.T.: 'Beamsteering in pattern reconfigurable arrays using directional modulation', *IEEE Trans. Antennas Propag.*, 2010, **58**, (7), pp. 2259–2265

[4] Hong, T., Song, M.Z., Liu, Y.: 'Dual-beam directional modulation technique for physical-layer secure communication', *IEEE Antennas Wirel. Propag. Lett.*, 2011, **10**, pp. 1417–1420

[5] Daly, M.P., Bernhard, J.T.: 'Directional modulation technique for phased arrays', *IEEE Trans. Antennas Propag.*, 2009, **57**, (9), pp. 2633–2640

[6] Daly, M.P., Bernhard, J.T.: 'Directional modulation and coding in arrays'. 2011 IEEE Int. Symp. on Antennas and Propagation (APSURSI), Spokane, WA, USA, July 2011, pp. 1984–1987

[7] Shi, H.Z., Tennant, A.: 'Enhancing the security of communication via directly modulated antenna arrays', *IET Microw. Antennas Propag.*, 2013, **7**, (8), pp. 606–611

[8] Ding, Y., Fusco, V.: 'Directional modulation transmitter synthesis using particle swarm optimization'. Proc. Loughborough Antennas and Propagation Conf., Loughborough, UK, November 2013, pp. 500–503

[9] Ding, Y.,, Fusco, V.: 'Directional modulation far-field pattern separation synthesis approach', *IET Microw. Antennas Propag.*, 2014, **9**, (1), pp. 41–48

[10] Ding, Y., Fusco, V.: 'Directional modulation transmitter radiation pattern considerations', *IET Microw. Antennas Propag.*, 2013, **7**, (15), pp. 1201–1206

[11] Zhu, Q.J., Yang, S.W., Yao, R.L., *et al.*: 'Directional modulation based on 4-D antenna arrays', *IEEE Trans. Antennas Propag.*, 2014, **62**, (2), pp. 621–628

[12] Litwin, L., Pugel, M.: 'The principles of OFDM', *RF Signal Process.*, 2001, **2**, pp. 30–48

[13] Chakravarthy, V., Nunez, A. S., Stephens, J. P., *et al.*: 'TDCS, OFDM, and MC-CDMA: a brief tutorial', *IEEE Commun. Mag.*, 2005, **43**, (9), pp. S11–S16

[14] Cho, Y.S., Kim, J., Yang, W.Y., *et al.*: '*Introduction to OFDM*' (Wiley-IEEE Press, 2010), pp. 111–151

[15] Hanzo, L., Akhtman, Y., Wang, L., *et al.*: '*Introduction to OFDM and MIMO-OFDM*' (Wiley-IEEE press, 2011), pp. 1–36

[16] Zhang, B., Liu, W., Gou, X.: 'Compressive sensing based sparse antenna array design for directional modulation', *IET Microw. Antennas Propag.*, 2017, **11**, (5), pp. 634–641

[17] Hawes, M. B., Liu, W.: 'Compressive sensing based approach to the design of linear robust sparse antenna arrays with physical size constraint', *IET Microw. Antennas Propag.*, 2014, **8**, (10), pp. 736–746

[18] Moffet, A.: 'Minimum-redundancy linear arrays', *IEEE Trans. Antennas Propag.*, 1968, **16**, (2), pp. 172–175

[19] Trees H.L., Van: '*Optimum array processing, part IV of detection, estimation, and modulation theory*' (Wiley, New York, 2002)

[20] Haupt, R.L.: 'Thinned arrays using genetic algorithms', *IEEE Trans. Antennas Propag.*, 1994, **42**, (7), pp. 993–999

[21] Yan, K.K., Lu, Y.: 'Sidelobe reduction in array-pattern synthesis using genetic algorithm', *IEEE Trans. Antennas Propag.*, 1997, **45**, (7), pp. 1117–1122

[22] Cen, L., Yu, Z.L., Ser, W., *et al.*: 'Linear aperiodic array synthesis using an improved genetic algorithm', *IEEE Trans. Antennas Propag.*, 2012, **60**, (2), pp. 895–902

[23] Trucco, A., Murino, V.: 'Stochastic optimization of linear sparse arrays', *IEEE J. Ocean. Eng.*, 1999, **24**, (3), pp. 291–299
[24] Prisco, G., D'Urso, M.: 'Exploiting compressive sensing theory in the design of sparse arrays'. Proc. IEEE Radar Conf., Kansas City, MO, USA, May 2011, pp. 865–867
[25] Carin, L.: 'On the relationship between compressive sensing and random sensor arrays', *IEEE Antennas Propag. Mag.*, 2009, **51**, (5), pp. 72–81
[26] Cen, L., Ser, W., Cen, W.*, et al.*: 'Linear sparse array synthesis via convex optimization'. Proc. IEEE Int. Symp. on Circuits and Systems, Paris, France, May 2010, pp. 4233–4236
[27] Oliveri, G., Massa, A.: 'Bayesian compressive sampling for pattern synthesis with maximally sparse non-uniform linear arrays', *IEEE Trans. Antennas Propag.*, 2010, **59**, (2), pp. 467–481
[28] Oliveri, G., Carlin, M., Massa, A.: 'Complex-weight sparse linear array synthesis by Bayesian compressive sampling', *IEEE Trans. Antennas Propag.*, 2012, **60**, (5), pp. 2309–2326
[29] Shen, Q., Liu, W., Cui, W.*, et al.*: 'Low-complexity direction-of-arrival estimation based on wideband co-prime arrays', *IEEE Trans. Audio Speech Lang. Process.*, 2015, **23**, (9), pp. 1445–1456
[30] Candès, E. J., Wakin, M. B., Boyd, S. P.: 'Enhancing sparsity by reweighted l_1 minimization', *J. Fourier Anal. Appl.*, 2008, **14**, pp. 877–905
[31] Prisco, G., D'Urso, M.: 'Maximally sparse arrays via sequential convex optimizations', *IEEE Antennas Wirel. Propag. Lett.*, 2012, **11**, pp. 192–195
[32] Fuchs, B.: 'Synthesis of sparse arrays with focused or shaped beampattern via sequential convex optimizations', *IEEE Trans. Antennas Propag.*, 2012, **60**, (7), pp. 3499–3503
[33] Grant, M., Boyd, S.: 'Graph implementations for nonsmooth convex programs', in Blondel, V., Boyd, S., Kimura, H. (Eds): '*Recent advances in learning and control, lecture notes in control and information sciences*' (Springer-Verlag Limited, 2008), pp. 95–110, http://stanford.edu/boyd/graph_dcp.html
[34] CVX Research: CVX: Matlab software for disciplined convex programming, version 2.0 beta. http://cvxr.com/cvx, September 2012